J Mater Sci (2010) 45:5547–5552
DOI 10.1007/s10853-010-4615-0

Stability of the nitrogen-deficient Ti_2AlN_x MAX phase in Ar^{2+}-irradiated (Ti,Al)N/Ti_2AlN_x multilayers

M. Bugnet · T. Cabioc'h · V. Mauchamp · Ph. Guérin · M. Marteau · M. Jaouen

Received: 13 February 2010 / Accepted: 11 May 2010 / Published online: 3 June 2010
© Springer Science+Business Media, LLC 2010

Abstract The effects of 100 keV Ar^{2+} ion irradiation on the structure and stability of multilayered dc sputtered and annealed thin films of (Ti,Al)N/Ti_2AlN_x have been investigated with X-ray diffraction and transmission electron microscopy. It is shown that the multilayer structure is preserved as well as the crystalline structures of both components. This demonstrates a high tolerance of the Ti_2AlN_x MAX phase in multilayers to damage induced by nuclear elastic interactions. It is suggested that damage recovery may originate from native nitrogen vacancies and from the interfaces that act as sinks for point defects, like Frenkel pairs, created during the irradiation.

Introduction

MAX phases form a group of nanolayered compounds with chemical formula $M_{n+1}AX_n$ with $n = 1$, 2, or 3, where M is an early transition metal, A is an A-group element (mostly IIIA and IVA), and X is either C and/or N. These layered ternary compounds combine both ceramic and metallic properties [1], and exhibit excellent thermal and mechanical properties [2, 3]. Their synthesis, under a thin film form, has been extensively studied in the last 10 years [3]. Concerning specifically the synthesis of Ti_2AlN, the MAX phase here studied, single-phased thin films were demonstrated to grow by reactive magnetron sputtering at temperatures higher than 675 °C [3–8]. Also, even though MAX phase layers can be directly deposited in a multilayered structure by magnetron sputtering [9] or by reactive CVD [10], multilayers can be a way to induce the nucleation of Ti_2AlN layers from temperatures as low as 500 °C [11–13]. In particular, the annealing of TiN/TiAl(N) multilayers was shown to lead to the formation of (Ti,Al)N/Ti_2AlN_x multilayers from 600 °C, in which the (Ti,Al)N layers have the cubic structure of TiN while the Ti_2AlN_x MAX phase layers are nitrogen deficient [13].

Recently, thanks to their exceptional thermal and mechanical properties, MAX phases have attracted attention for potential applications as structural materials in nuclear reactors. Indeed nuclear fission and fusion reactors require materials that can survive extreme environments such as high irradiation rate, high temperature, oxidation, and stress. However, up to now, little is known about the MAX phases behavior under irradiation. As far as authors know, only three different studies have been reported about the MAX phases behavior under ion irradiation [14–16]. They are all related to heavy ion irradiation, at energies in the order of some tens of MeV, in 312 compounds Ti_3SiC_2, $Ti_3Si_{0.90}Al_{0.10}C_2$, and $Ti_3(Si,Al)C_2$. In particular, the work of Nappé et al. allowed to consider irradiation damage induced by nuclear elastic and electronic inelastic interactions at room temperature in Ti_3SiC_2 [14]. Concerning elastic collisions, a preferential sputtering of the surface is observed as a function of the crystallite orientation and an amorphisation phenomenon occurred for a fluence of 10^{14} Au/cm^2. On the other hand, electronic interactions are shown to induce the formation of hills, an expansion of the c lattice parameter and a partial amorphisation from 10^{15} Xe/cm^2. Interestingly Liu et al. evidenced an expansion along the c axis, the appearance of microstrains, but, contrary to the work dedicated to Ti_3SiC_2 [14], no clear occurrence of amorphisation in $Ti_3Si_{0.90}Al_{0.10}C_2$ up to

M. Bugnet (✉) · T. Cabioc'h · V. Mauchamp · Ph. Guérin · M. Marteau · M. Jaouen
Département Physique et Mécanique des Matériaux, Institut Pprime, UPR 3346 CNRS, Université de Poitiers, ENSMA, SP2MI, Téléport 2, Boulevard Marie et Pierre Curie, BP 30179, 86962 Futuroscope Chasseneuil Cedex, France
e-mail: matthieu.bugnet@etu.univ-poitiers.fr

2×10^{15} Xe/cm^2 [15]. Also a TEM investigation of Xe-irradiated $Ti_3(Si,Al)C_2$ by Le Flem et al. confirmed a retained crystalline structure up to 2×10^{15} Xe/cm^2 without amorphisation and also showed the apparition of hills at the surface.

Even though carbides seem to be cladding materials of choice for future fuels of gas cooled fast reactors, nitrogen-based MAX phases shall also be considered from a fundamental point of view. As shown in previous work [13], the induced transformation of (Ti,Al)N/Ti_2AlN_x multilayers is a way to synthesize the Ti_2AlN_x MAX phase. Also, because of their low thickness (typically a few hundred nm), thin films such as (Ti,Al)N/Ti_2AlN_x multilayers are very well designed for low energy ion irradiation experiments. Furthermore, no information is reported about low energy ($\sim$100 keV) ion irradiation of MAX phases. Therefore, the primary aim of this article is to investigate the resistance to damage induced by nuclear interactions in the (Ti,Al)N/Ti_2AlN_x multilayer system and especially to focus on the stability of the Ti_2AlN_x layers.

Experimental details

In a first step, a TiN/TiAl(N) multilayer was deposited at room temperature onto a single crystalline (100) silicon wafer using a computer controlled NORDIKO-3000 dual ion beam sputtering system (the notation TiAl(N) indicates that TiAl layers contain some nitrogen). The details of the deposition setup can be found in reference 13. In the present study, the $[TiN_{6\ nm}/TiAl(N)_{10\ nm}]_5$ multilayer consists of five periods of alternate TiN and amorphous TiAl(N) layers with a modulation wavelength $\Lambda = t_{TiN} + t_{TiAl(N)} = 16$ nm, the thicknesses of the TiN and TiAl(N) layers being, respectively: $t_{TiN} = 6$ nm and $t_{TiAl(N)} = 10$ nm. The deposition starts with a TiN layer and a 6-nm thick TiN capping is added at the end (total thickness of the film: 86 nm) to prevent TiAl oxidation during annealing. The as-prepared multilayer was then annealed in vacuum at 720 °C for 150 min (pressure: 10^{-4} Pa) resulting in the formation of a (Ti,Al)N/Ti_2AlN_x multilayer [13]. It should be noted here that the so obtained MAX phase is expected to be nitrogen deficient. Indeed, a 0.53 nitrogen atomic ratio was measured for an annealing temperature of 600 °C [13]. This ratio should be of the same order of magnitude for an annealing temperature of 720 °C, which was chosen to promote a better crystallization of the Ti_2AlN_x layers. It is also worth mentioning that the nucleation of the MAX phase is accompanied with an expansion of the TiAl(N) layers, the TiN layers kept their initial thickness of 6 nm and the film was about 120-nm thick after annealing. The sample was then irradiated with Ar^{2+} ions at room temperature using an ion implanter EATON operating at a base pressure of 10^{-5} Pa. The ion current density was kept below 0.4 μA/cm^2 to prevent sample heating, and the Ar^{2+} ions were accelerated up to 50 kV (energy: 100 keV). This energy value was selected on the basis of SRIM simulations [17] with an ion projected range slightly exceeding the total film thickness, as illustrated in Fig. 1. The corresponding primary recoil energy was 57 eV/ion/Å on average, and the multilayers were successively irradiated at different ion fluences ranging from 1.8×10^{13} up to 1.8×10^{15} Ar/cm^2. The highest fluence corresponds to a maximum dose of approximately 12 displacements per atom, assuming an average threshold energy of 30 eV.

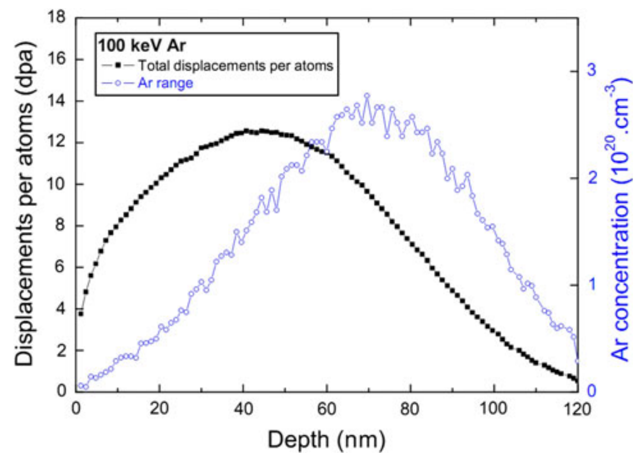

Fig. 1 SRIM simulations of Argon concentration and damage profile induced in (Ti,Al)N/Ti_2AlN_x by 100 keV Ar^{2+} ions for a fluence of 1.8×10^{15} Ar/cm^2 [17]

To investigate the microstructure of the multilayers, X-ray diffraction (XRD) characterizations were performed in the Bragg–Brentano geometry, in the 2θ range between 20° and 56°, using a Bruker D8 diffractometer (Cu K_α source, 40 kV, 40 mA). In such geometry and large angles, the depth investigated by X-ray is much deeper than the thickness of the film, the latter being thus entirely probed. The measured XRD patterns before and after irradiation for ion fluences ranging from 1.8×10^{13} to 1.8×10^{15} Ar/cm^2 are shown in Fig. 2. Transmission Electron Microscopy (TEM) cross sections were examined with a TEM JEOL 2200FS microscope operating at 200 kV. An in column Ω filter enables the chemical analysis by Electron Energy-Loss Spectroscopy (EELS). Spectra were dark count corrected and deconvoluted from multiple scattering using a Fourier-Ratio technique [18].

Results and discussion

After thermal annealing (spectrum at the bottom of Fig. 2), the sample exhibits several diffraction peaks related to TiN and Ti_2AlN. One also notes two additional peaks located at

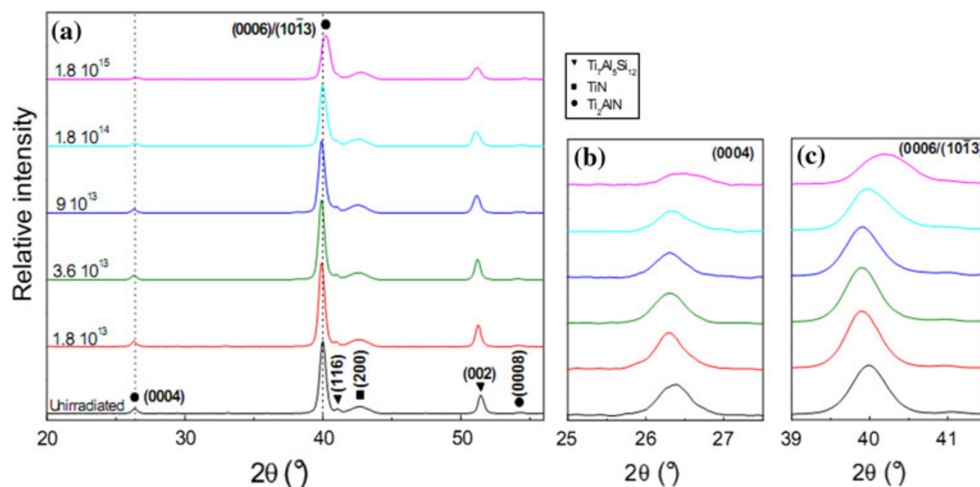

Fig. 2 XRD diagram from the (Ti,Al)N/Ti_2AlN_x multilayer structure annealed at 720 °C as a function of the fluence (units Ar/cm^2), the *dotted line* is a guide for eyes (**a**); magnification around the Ti_2AlN_x (0004) and $(0006)/(10\bar{1}3)$ diffraction peak (**b**) and (**c**)

$2\theta \sim 41°$ and $2\theta \sim 51°$ which may be attributed to the (116) and (200) reflections of the ternary compound $Ti_7Al_5Si_{12}$ [19]. This last phase can simply originate from the diffusion of some Ti and Al atoms inside the silicon substrate. One can observe a single texture (200) for TiN, as it was already the case before annealing. For Ti_2AlN, the diffraction peak at an angle of $2\theta = 26.37°$ stems from the (0004) reflection, and one can think that Ti_2AlN_x phase is textured according to the (000ℓ) planes. The angular position of this peak corresponds to a value of the *c* lattice parameter of (13.52 ± 0.01) Å, a value lower than the bulk one (13.62 Å [20]). This points out for a possible compressive stress along the *c* axis and, due to Poisson effect, for tensile stress in the basal planes. This low *c* value may also arise in part from a non-negligible amount of vacancies on the N-sites. The diffraction peak at $2\theta = 40°$ can be attributed to a mix-up of the reflections on the (0006) and $(10\bar{1}3)$ planes, the $(10\bar{1}3)$ reflection being referred as the most intense.

A typical bright field cross-sectional TEM micrograph of the 720 °C annealed multilayer, prior to ion irradiation, is shown in Fig. 3a. The total thickness (120 nm) of stack is larger than for the as deposited one (86 nm). Whereas the thickness of the TiN sub-layers corresponds to the as deposited one (6 nm), the Ti_2AlN_x sub-layers are much thicker than 10 nm: their average thickness is 16 nm. The major contribution to this expansion originates from the phase transformation of the amorphous TiAl(N) into the hexagonal Ti_2AlN_x during annealing. Furthermore one can observe that TiN grains are clearly visible in the top half of the multilayer structure, whereas the contrasts of the grains close to the substrate disappear. Therefore, the 50 nm closer to the substrate appear to be strongly perturbed, particularly the second Ti_2AlN_x-based layer which is much thicker than the other ones. It likely comes from diffusion processes during annealing between the substrate and the film, the nitrogen deficient first TiN layer being not efficient enough as a barrier of diffusion [13]. A slight diffusion of some Al and Ti atoms toward the silicon substrate could be responsible for these perturbed TiN and Ti_2AlN_x sub-layers close to the substrate. This last point is confirmed by the observation of some $Ti_7Al_5Si_{12}$ grains at the multilayer/Si interface (not shown here).

However, Si diffusion cannot explain the anomalously thick second Ti_2AlN_x layer because the related EELS spectrum (Fig. 3b) clearly reveals the nitrogen *K* edge at 400 eV and titanium L_{23} edges at 455 eV while the silicon L_{23} edges (∼100 eV) were not observed in this area. In short, the questions raised by the inter-diffusion processes occurring during annealing at the film/silicon interface are not yet fully understood but are beyond the scope of this article. EELS measurements were also performed to investigate the chemical composition of the grains. Unfortunately due to the important roughness of the interfaces it is very difficult to quantify the chemical composition of the Ti_2AlN_x layers because of some TiN grains leaking under the Ti_2AlN_x ones. Even if the values for the Ti/N ratio vary between 2 and 2.5, no precise value of *x* can be given from these measurements. In particular, it is not sure that the Ti_2AlN_x sub-layers characterized in this study are as nitrogen deficient as it was unambiguously the case after thermal annealing at 600 °C of similar multilayers [13].

To have a better insight of the microstructure of the multilayers, High Resolution TEM (HRTEM) observations of this cross-section were achieved. A typical micrograph is shown in Fig. 3c as well as the Fast Fourier Transform (FFT) corresponding to the zone indicated by the square in inset. One can clearly identify on this FFT the (000ℓ) spots typical of the MAX phase. The *c* lattice parameter deduced from this FFT is 13.5 ± 0.1 Å, a value in good agreement with the one deduced from XRD measurements.

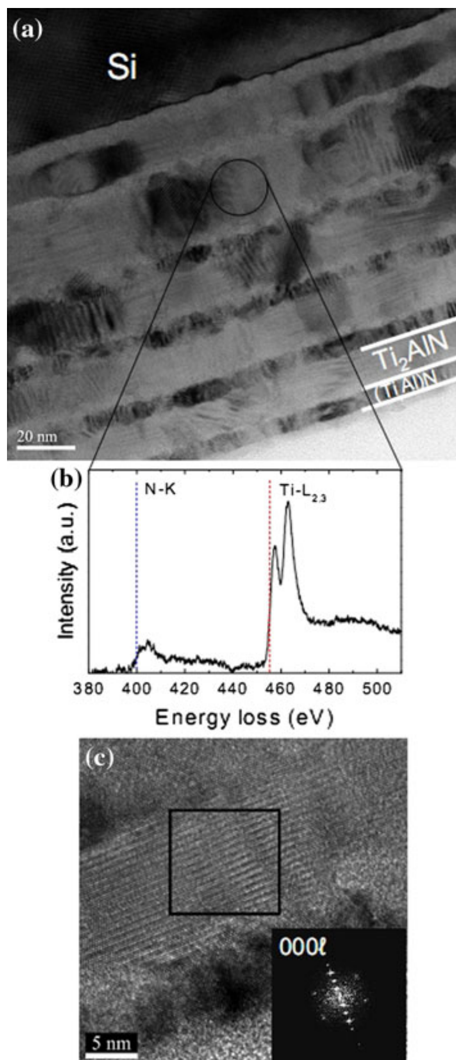

Fig. 3 Bright field X view of the annealed $[TiN_{6\ nm}/TiAl(N)_{10\ nm}]_5$ multilayer (**a**); high energy-loss EELS spectrum of the area indicated by the *circle* (energy range: 380–510 eV) (**b**); HRTEM of the 720 °C annealed $[TiN_{6\ nm}/TiAl(N)_{10\ nm}]_5$ multilayer showing a Ti_2AlN grain (Inset: FFT of the area indicated by the *square*) (**c**)

The resistance to irradiation damage of the multilayer was characterized by XRD and cross-sectional TEM observations on the same sample irradiated with a fluence increasing from 1.8×10^{13} to 1.8×10^{15} Ar/cm^2. On the XRD pattern shown in Fig. 2a, one can observe that the angular positions of the Ti_2AlN_x (0004) and $(0006)/(10\bar{1}3)$ diffraction peaks vary when the fluence is increased. After the lowest fluence, both Ti_2AlN_x peaks move slightly toward lower angles as it is clearly shown in Fig. 2b, c. Based on the angular positions of the (0002) (not shown here) and (0004) reflections, we find that c increases from (13.52 ± 0.01) Å (virgin) up to $(13{,}55 \pm 0.01)$ Å (1.8×10^{13} Ar/cm^2). Even if c remains far from the bulk value, such a phenomenon clearly reveals a relaxation of the internal stresses induced by thermal annealing. For larger fluences, on the opposite, these peaks are shifted toward larger angles indicating a decreasing of the c parameter that ends at 13.46 ± 0.01 Å. A so low value is difficult to explain: one can evoke the existence of native N vacancies that precipitate in vacancies loops under irradiation resulting in a collapse of the structure along the c axis, but it remains an assumption quite difficult to confirm from TEM observations owing to the overlap and limited size of the Ti_2AlN_x grains. Furthermore the intensities of the Ti_2AlN_x (0004) and $(0006)/(10\bar{1}3)$ diffraction peaks decrease as the fluence is increased from 9×10^{13} to 1.8×10^{15} Ar/cm^2. This phenomenon is accompanied by a slight broadening of the peaks Full Width Half Maximum (FWHM) (see Fig. 1b). These two observations indicate the creation of micro-distorsions inside the layers and/or a small decrease of the finite size of the coherent domains of diffraction in the direction of growth. Nevertheless, as demonstrated by the presence of the diffraction peaks, one can already conclude that Ti_2AlN_x grains survive a damage rate as high as 12 dpa. We can therefore safely exclude a significant amorphisation of the MAX phase, an observation in good agreement with high energy ion irradiation of $Ti_3Si_{0.9}Al_{0.1}C_2$ and $Ti_3(Si,Al)C_2$ from Liu et al. and Le Flem et al. [15, 16].

More informations on the microstructure of the multilayer after irradiation were obtained from a cross-sectional TEM observation of the sample irradiated with the largest fluence (1.8×10^{15} Ar/cm^2). On the typical bright field cross-sectional view shown in Fig. 4a, one can observe that the multilayer structure remains unchanged. Indeed, the diffraction contrasts and the modulation length are similar to those observed prior to irradiation (Fig. 3a). Figure 4b, c shows HRTEM micrographs obtained in Ti_2AlN_x sublayers with the FFT corresponding to the area inside the square in inset. This leads to the lattice parameter values $a = (3.0 \pm 0.1)$ Å, in good agreement with the reported value $a = 2.99$ Å [20], and $c = (13.3 \pm 0.1)$ Å. Concerning the c parameter it is lower than the value prior to irradiation, $c = (13.52 \pm 0.01)$ Å. Such a reduction of the c parameter with increasing doses is in good agreement with XRD measurements. The presences of Ti_2AlN_x as well as the remaining multilayer structure are thus entirely confirmed by the HRTEM.

For the last decades, TiN has been extensively investigated as a coating for improved tribological properties. Recently, it was also studied for its structural, thermal, and electro-conductive properties [21–23], its ability as diffusion barrier [24] or the effect of MoS_x addition on its wear resistance properties [25]. The effects of ion implantation and irradiation in TiN single phase coatings have also been investigated to study the influence of grain size effect [26], residual stresses [27], wear [28], or hardness improvement [29]. As a general trend, it turns out that TiN is strongly

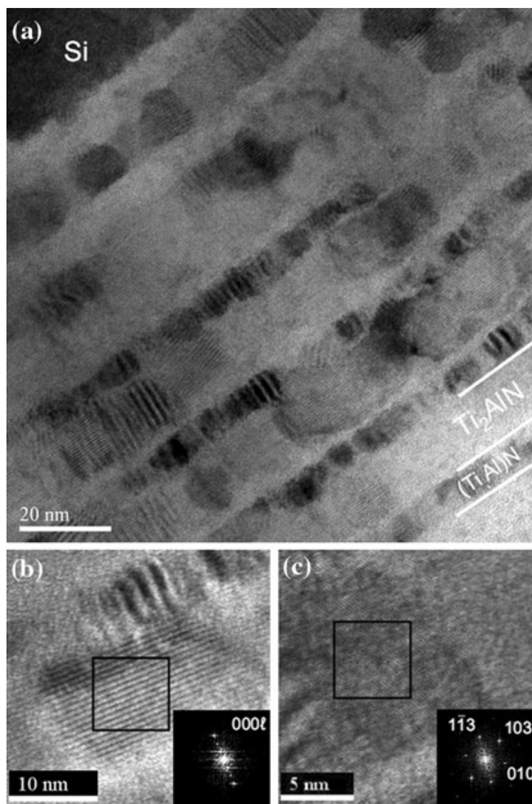

Fig. 4 Bright field X view of the (Ti,Al)N/Ti_2AlN_x multilayer after ion irradiation at a fluence of 1.8 × 10^{15} Ar/cm^2 (**a**) and HRTEM of two differently orientated Ti_2AlN_x grains after ion irradiation at a fluence of 1.8 × 10^{15} Ar/cm^2 (Inset: FFT of the area indicated by the *square*) (**b**, **c**)

resistant toward ion irradiation damage. The behavior under irradiation of a wide range of multilayer systems containing TiN has been studied so far. They dealt with structural modifications, interface mixing and stresses induced by irradiation [30–33]. More generally, ion irradiation effects in multilayers were intensively investigated to study ion-induced stresses relaxation and mixing at interfaces [34–37]. Figure 2 shows that the (Ti,Al)N (200) diffraction peak is almost unaffected by the irradiation, whatever the fluence. This result is in good agreement with previously reported studies about ion irradiation of TiN, either as coatings [26] or as multilayers [30, 33]. This clearly displays the strong stability of (Ti,Al)N with respect to ion irradiation induced damages.

Ti_2AlN_x appears to be highly tolerant to Ar ion irradiation. However, this behavior might be exacerbated by different aspects. First, the interfaces in the multilayer structure are known to be generally more irradiation resistant than the bulk counterparts [38]. Indeed interfaces in nanometric systems, such as Cu/Nb nanocomposites, play a crucial role as pathways for diffusion of implanted species and enhance the annihilation of vacancies and interstitials induced by irradiation [38, 39]. Second, one cannot exclude the effect of diffusion process between the film and the substrate. Finally native nitrogen vacancies should contribute to the important tolerance to irradiation damage. Indeed the vacancies initially present in the lattice and those induced by collision cascades could provide additional contributions to the annihilation of Frenkel pairs as well as the creation of Ar-vacancy complexes. In order to check the validity of this latter hypothesis, the deposition of N-deficient single-phased Ti_2AlN_x thin films should be performed for irradiation purposes. This remains a challenge since only the synthesis of stoichiometric Ti_2AlN is currently controlled [3–8].

Conclusion

The behavior of a (Ti,Al)N/Ti_2AlN_x multilayer structure was investigated under 100 keV Ar^{2+} ion irradiation at room temperature. XRD in Bragg–Brentano geometry and TEM evidenced a strong tolerance of Ti_2AlN_x with respect to ion irradiation damage induced by nuclear elastic collisions, the multilayer structure being conserved for fluences up to 1.8 × 10^{15} Ar/cm^2. It is shown that Ti_2AlN_x does not seem to be sensitive to amorphisation up to a dose of 1.8 × 10^{15} Ar/cm^2 and the MAX phase nanolaminated structure is retained. This study of ion irradiated Ti_2AlN_x shows promising results for further investigations of the behavior of nitride based MAX phases under ion irradiation.

References

1. Barsoum MW (2000) Prog Solid State Chem 28:201
2. Wang J, Zhou Y-C (2009) Annu Rev Mater Res 39:415
3. Eklund P, Beckers M, Jansson U, Högberg H, Hultman L (2010) Thin Solid Films 518:1851
4. Beckers M, Höglund C, Baehtz C, Martins RMS, Persson POÅ, Hultman L, Möller W (2009) J Appl Phys 106:064915
5. Joelsson T, Flink A, Birch J, Hultman L (2007) J Appl Phys 102:074918
6. Beckers M, Schell N, Martins RMS, Mücklich A, Möller W, Hultman L (2007) J Appl Phys 102:074916
7. Magnuson M, Mattesini M, Li S, Höglund C, Beckers M, Hultman L, Eriksson O (2007) Phys Res B 76:195127
8. Persson POÅ, Kodambaka S, Petrov I, Hultman L (2007) Acta Mater 55:4401
9. Wilhelmsson O, Eklund P, Giuliani F, Högberg H, Hultman L, Jansson U (2007) Appl Phys Lett 91:123124
10. Fakih H, Jacques S, Berthet MP, Bosselet F, Dezellus O, Viala JC (2006) Surf Coat Technol 201:3748
11. Borysiewicz MA, Kaminska E, Piotrowska A, Pasternak I, Jakiela R, Dynowska E (2008) Acta Phys Pol A 114:1061
12. Höglund C, Beckers M, Schell N, Borany JV, Birch J, Hultman L (2007) Appl Phys Lett 90:174106

13. Dolique V, Jaouen M, Cabioc'h T, Pailloux F, Guérin Ph, Pélosin V (2008) J Appl Phys 103:083527
14. Nappé JC, Grosseau Ph, Audubert F, Guilhot B, Beauvy M, Benabdesselam M, Monnet I (2009) J Nucl Mater 385:304
15. Liu X, Le Flem M, Béchade J-L, Onimus F, Cozzika T, Monnet I (2010) Nucl Instrum Methods Phys Res B 268:506–512
16. Le Flem M, Liu X, Doriot S, Cozzika T, Monnet I (2010) Int J Appl Ceram Tech (accepted)
17. Ziegler JF, Biersack JP, Littmark U (1985) The stopping and range of ions in solids. Pergamon, New York. http://www.srim.org
18. Egerton RF (1986) Electron energy-loss spectroscopy in the electron microscope. Plenum Press, New York
19. Raman A, Schubert K (1965) Z Metallkde 56:45
20. Hug G, Jaouen M, Barsoum MW (2005) Phys Rev B 71:024105
21. Peruško D, Mitric M, Milinović V, Petrović S, Miloslavjević M (2008) J Mater Sci 43:2625. doi:10.1007/s10853-008-2477-5
22. Albert Irudayaraj A, Srinivasan R, Kuppusami P, Mohandas E, Kalainathan S, Ramachandran K (2008) J Mater Sci 43:1114. doi:10.1007/s10853-007-2248-8
23. Ohzawa Y, Cheng X, Achiha T, Nakajima T, Groult H (2008) J Mater Sci 43:2812. doi:10.1007/s10853-008-2537-x
24. Roger J, Audubert F, Le Petitcorps Y (2010) J Mater Sci 45:3073. doi:10.1007/s10853-010-4314-x
25. Haider J, Rahman M, Hashmi MSJ, Sarwar M (2008) J Mater Sci 43:3368. doi:10.1007/s10853-008-2471-y
26. Wang H, Araujo R, Swadener JG, Wang YQ, Zhang X, Fu EG, Cagin T (2007) Nucl Instrum Methods Phys Res B 261:1162
27. Perry AJ (1998) Mater Sci Eng A 253(1–2):310
28. Oda K, Nakayama A, Ohara H, Kitagawa N, Nomura T (1997) Nucl Instrum Methods Phys Res B 121:283
29. Sansom D, Viviente JL, Alonso F, Ugarte JJ, Oate JI (1996) Surf Coat Technol 84(1–3):519
30. Miloslavljević M, Peruško D, Milinović V, Stojanović Z, Zalar A, Kovać J, Jeynes C (2010) J Phys D 43:065302
31. Peruško D, Webb MJ, Milinović V, Timotijević B, Miloslavjević M, Jeynes C, Webb RP (2008) Nucl Instrum Methods Phys Res B 266(8):1749
32. Hübler R (2001) Nucl Instrum Methods Phys Res B 175–177:630
33. Fayeulle S, Torri P, Nastasi M, Lu YC, Kung H, Tesmer JR (1997) Nucl Instrum Methods Phys Res B 127–128:198
34. Jaouen M, Pacaud J, Jaouen C (2001) Phys Rev B 64:144106
35. Martin F, Jaouen C, Pacaud J, Abadias G, Djemia Ph, Ganot F (2005) Phys Rev B 71:045422
36. Debelle A, Michel A, Abadias G, Jaouen C (2006) Nucl Instrum Methods Phys Res B 242(1–2):461
37. Abadias G, Michel A, Tromas C, Jaouen C, Dub SN (2007) Surf Coat Technol 202(4–7):844
38. Zhang X, Li N, Anderoglu O, Wang H, Swadener JG, Höchbauer T, Misra A, Hoagland RG (2007) Nucl Instrum Methods Phys Res B 261(1–2):1129
39. Demkowicz MJ, Hoagland RG, Hirth JP (2008) Phys Rev Lett 100:136102